0 0 0 0 4 2 0 7 3 1 1

Submitted to Nuclear Science and Engineering

LBL-3551 Rev.
Preprint c. 1

DESIGN OF IDEAL CASCADES OF GAS CENTRIFUGES WITH VARIABLE SEPARATION FACTORS

D. R. Olander

RECEIVED
LAWRENCE
BERKELEY LABORATORY

OCT 24 1975

LIBRARY AND
DOCUMENTS SECTION

September 1975

Prepared for the U. S. Energy Research and Development Administration under Contract W-7405-ENG-48

For Reference

Not to be taken from this room

LAWRENCE BERKELEY LABORATORY
UNIVERSITY OF CALIFORNIA
BERKELEY

LBL-3551 Rev.
c. 1

DISCLAIMER

This document was prepared as an account of work sponsored by the United States Government. While this document is believed to contain correct information, neither the United States Government nor any agency thereof, nor the Regents of the University of California, nor any of their employees, makes any warranty, express or implied, or assumes any legal responsibility for the accuracy, completeness, or usefulness of any information, apparatus, product, or process disclosed, or represents that its use would not infringe privately owned rights. Reference herein to any specific commercial product, process, or service by its trade name, trademark, manufacturer, or otherwise, does not necessarily constitute or imply its endorsement, recommendation, or favoring by the United States Government or any agency thereof, or the Regents of the University of California. The views and opinions of authors expressed herein do not necessarily state or reflect those of the United States Government or any agency thereof or the Regents of the University of California.

0 0 0 0 4 2 0 7 8 1 2

LBL-3551 Rev.

DESIGN OF IDEAL CASCADES OF GAS CENTRIFUGES WITH VARIABLE SEPARATION FACTORS

by D. R. Olander

Inorganic Materials Research Division of the
Lawrence Berkeley Laboratory and the
Department of Nuclear Engineering of the
University of California
Berkeley, California 94720

ABSTRACT

A method of designing ideal cascades in which the separation factor varies with stage number is presented and applied to centrifuges as separating units. The centrifuge is characterized by a performance function, which gives the separative power, optimized with respect to all internal variables, as a function of cut and throughput. For centrifuges with certain types of performance functions, variable-α ideal cascades can provide product at lower cost than the conventional ideal cascade in which the separation factor is independent of stage number.

1. Introduction

As far as is known, all cascades for uranium isotope separation are designed as ideal cascades with all separating units operated in exactly the same manner. When the separation factor (or the separative power) does not vary with stage number, the characteristics of the ideal cascade may be obtained from the theory developed in the books by Cohen (1) and Benedict and Pigford (2). However, we show in this paper that it is possible to construct ideal (i.e., no-mixing) cascades in which the separation factor varies from stage to stage. For certain types of separating units, the performance of this "variable-α" ideal cascade is superior to that of the conventional "constant-α" ideal cascade.

In order to attain the no-mixing condition at each point in the cascade where streams join, each separating unit in a constant-α cascade must be operated symmetrically. In symmetric operation, the heads separation factor α is equal to the tails separation factor β. In a variable-α ideal cascade, on the other hand, the no-mixing requirement imposes different constraints on the asymmetries of the units in adjacent stages.

The ability of a centrifuge to perform as an isotope separator is described by the dependence of some measure of its separative efficiency (e.g., heads, tails, or total separation factor or separative power) as a function of all experimentally controllable variables. The latter may be divided into two classes: internal parameters and operating parameters. The distinction between the two classes is as follows: changing an internal parameter affects only the product and waste compositions but does not alter the feed, product or waste flow rates. Change of an operating variable disrupts both the flows and compositions of the streams leaving the centrifuge. The two operating variables are the cut θ and the

throughput L. Among the internal parameters are the temperature differences across the end caps of the rotor and the design and position of any scoops inside the rotor. The geometry (height and radius) and peripheral speed of the rotor are not considered to be controllable variables. The rotor is always driven close to its strength or stability limit; there is no reason to do otherwise.

Throughout this analysis, we assume that the isotope fractions of U-235 in all streams are much smaller than unity. With this restriction, the heads separation factor for a single centrifuge is given by:

$$\alpha = x_p/x_F \tag{1}$$

where x_p is the U-235 concentration in the product stream and x_F is the feed composition. The tails separation factor is:

$$\beta = x_F/x_w \tag{2}$$

where x_w is the waste composition from the centrifuge. By means of material balances, the cut θ is found to be related to the separation factors by:

$$\theta = \frac{\beta - 1}{\alpha\beta - 1} \tag{3}$$

Theory and experiment give the separation factor as a function of all controllable parameters of the centrifuge, or by a function of the general form:

$$\alpha(L, \theta, \text{internal variables})$$

The centrifuge performs most efficiently when the internal variables are adjusted (at each combination of L and θ) so that the separation factor is a maximum. The optimized separation factor is therefore a function only of the operating variables

L and θ. Using an asterisk to denote optimization with respect to all internal variables, the function $\alpha^*(L,\theta)$ is called the performance function of the centrifuge. Provided all of the internal variables have been considered in the optimization process, the isotope separating capability of the centrifuge is completely defined by the performance function.

If the condition of symmetry ($\alpha=\beta$) is imposed upon the centrifuge because it is to be employed in a constant-α ideal cascade, Eq. (3) shows that $\theta = 1/(1 + \alpha)$, and hence α^* is a function of L only. However, for the variable-α cascade, the restriction $\alpha = \beta$ does not apply and knowledge of the complete (i.e., two-dimensional) performance function must be used in cascade analysis.

2. Centrifuge Flow Models

Three different centrifuge performance functions are utilized in comparing constant-α and variable-α cascades. All of the centrifuge models are derived by means of the Cohen method of solving the diffusion equation in the gas contained in the rotor (3). Brief summaries of the three models are presented below; additional details are given in Appendix I.

Case A is the original Cohen model, in which the axial flow velocity is independent of axial position in the centrifuge (i.e., the "long bowl" approximation). The only internal variable is the parameter m, which represents the ratio of the magnitude of the circulating flow to a characteristic molecular diffusion rate. Optimization with respect to this internal variable is accomplished by varying m until the separation factor is a maximum.

Cases B and C permit axial decay of the axial velocity profile. The radial shape of the axial velocity is assumed to be independent of axial position, and only the magnitude of the flow changes. The gradient equations derived by Cohen still apply, but the coefficients are dependent upon axial location. In case B, the internal flow is assumed to be driven thermally by a temperature difference at one end cap. The radial dependence of the axial velocity is taken from the calculations of Jacques (4), although the particular radial shape is not as important in the present analysis as is the fact that the flow decays with distance from the driving end cap. Exponential axial decay of the flow in a centrifuge rotor was predicted by Ging (5). However, we have utilized decay constants larger than that predicted by Ging's calculations in order to enhance the basic axial asymmetry about the midplane which this type of flow pattern causes. In case B, the only internal variable used in optimization is the end cap temperature difference, which is varied until α is maximized.

Case C represents a centrifuge driven thermally from both ends by temperature differences of opposite sign on the two end caps. As in case B, the radial shape of the end-driven flow is taken from Jacques' calculation and the flow magnitude is allowed to decrease with distance away from the appropriate driving end. In principle, both end cap temperature differences are internal variables which should be included in the optimization process. To avoid time-consuming optimization calculations, the ratio of the end cap temperature differences and the common axial decay constant are fixed, so that only one optimization parameter needs to be considered.

Figure 1 shows the variation of the magnitude of the axial flow velocity with height in the rotor for the three cases treated. The velocities have been normalized to unity at the bottom of the stripping section. The magnitude of the axial velocity is determined by the internal variable driving the flow (m for case A and the hot end cap temperature difference for cases B and C) which is varied in order to maximize the separation factor.

3. Performance Functions

The information contained in the performance function $\alpha^*(L,\theta)$ may be expressed in terms of other variables. The usual dependent variable is the separative power of the centrifuge, and the function $\delta U^*(L,\theta)$ may be obtained directly from $\alpha^*(L,\theta)$. The asterisk on δU indicates that it is optimized with respect to all internal variables. For cascade analysis, it is convenient to consider α and β as independent variables and L^* and δU^* as optimized dependent variables. If θ is expressed in terms of α and β by Eq. (3), the performance function $\alpha^*(L,\theta)$ can be turned inside out to yield the function $L^*(\alpha,\beta)$. Here L^* is the maximum throughput which can be achieved at specified values of α and β. It may be shown that the values of the internal variables which maximize α for a particular L,θ combination are the same as those which maximize L at specified α and β. Thus, $L^*(\alpha,\beta)$ is another way of expressing the performance function of the centrifuge.

Presentation and analytical application of the performance function is facilitated if the dependent variable is chosen as the separative power δU^* rather than the separation factor α^* or the throughput L^*. The reason for this is that δU^* varies much more slowly with either sets of independent variables (L,Θ) or (α,β) than do the other two possibilities. There is, however, disagreement concerning the proper formulation of the separative power for asymmetric elements.

Defining a function $f(\alpha,\beta)$ by:

$$f(\alpha,\beta) = \frac{\alpha(\beta-1)\ln\alpha - (\alpha-1)\ln\beta}{\alpha\beta - 1}, \tag{4}$$

Bulang et al (6) obtain the separative power:

$$\delta U = Lf(\alpha,\beta) \tag{5}$$

whereas Ouwerkerk and Los (7) arrive at the relation:

$$\delta U = Lf(\beta,\alpha) \tag{6}$$

Equation (6) may also be termed the Cohen separative power because it was obtained by Ouwerkerk and Los (7) assuming that the value function derived by Cohen (1) is applicable. [Use Eq.(III-18) in Eq. (10), express concentrations in terms of α and β by Eqs. (1) and (2) and eliminate the cut by Eq. (3).]

These two formulations apply to dilute concentrations of U-235 in U-238 and differ only in the order in which the variables α and β appear in the function f. Whether the separative power is described by Eq. (5) or by Eq. (6), $\delta U^*(\alpha,\beta)$ corresponds to the product of $L^*(\alpha,\beta)$ and either $f(\alpha,\beta)$ or $f(\beta,\alpha)$. The relative merits of these two expressions for the separative power of a single asymmetric separating unit will be discussed in Sec. 4. However, for the present analysis, Eq. (5) and Eq. (6) may be regarded simply as alternate means of describing the centrifuge performance function. The choice of Cohen's or Bulang's separative power is not important in the cascade calculations. As shown in the following section, cascade configurations are compared on the basis of a figure-of-merit which closely represents the cost per unit amount of a product of specified concentration.

The magnitudes of the optimized separative powers of the centrifuges modeled in the present calculation were not the main point of interest. The important aspect of the performance function is the manner in which δU^* varies with L and Θ or with α and β. Hence, the input parameters for the calculation of the flow fields were selected so as to be reasonably realistic and to yield separation factors sufficiently greater than unity so that the analytical degeneracies associated with close separation were avoided. In order to simplify the separation performance calculations, the range of the operating variables was restricted. The cut was required to be in the range $0.1 \leq \Theta \leq 0.9$ and the throughput was restricted to the range $L_{min} \leq L \leq L_{max}$. Our object is to compare constant-α and variable-α cascades comprised of centrifuges having the same performance function. The conclusions of this analysis are not substantially affected by restricting the range of operating variables to the confines cited above.

Figures 2, 3, and 4 show the performance functions δU^* in terms of the independent variables L and Θ (left hand panels) and in terms of α and β (right hand panels) for centrifuges A, B, and C. The performance functions $\delta U^*(\alpha,\beta)$ are presented as topographical maps in which the contours are lines of constant δU^*. Bulang's separative power (Eq. (5)) has been used in all plots. Had the Cohen separative power (Eq. (6)) been used instead, the curves in the left hand panels of Figs. 2-4 would have been somewhat flatter than those for Bulang's separative power and the contours in the right hand panels would have been somewhat altered. However, the qualitative features of the performance function plots would be the same and identical values of $L^*(\alpha,\beta)$ could be computed from them.

The left hand panels of Figures 2 - 4 display the performance functions as they normally would be obtained from experiment or from theoretical calculation. The case A performance function of Figure 2 indicates that δU^* is relatively insensitive to cut for $\theta < 0.6$ but thereafter decreases rapidly. The $\delta U^*(L,\theta)$ plot for the case B centrifuge (Figure 3) decreases uniformly with cut. This behavior reflects the decay of the axial velocity with distance from the heated end cap at the bottom of the stripping section. In order to avoid isotope mixing, the feed injection point in units of rotor length is approximately equal to the cut (in the close-separation limit, these two quantities are exactly equal (5)). Consequently, separative performance is improved to the extent that the feed can be introduced at an axial position where the circulatory flow is strong. For the case B centrifuge, feed injection near the bottom of the stripping section, which implies a small cut, produces the largest δU^*. In the case C centrifuge shown in Figure 4, the flow strength passes through a minimum at

$\theta = 0.4$ (Figure 1). As a result, when the cut (and hence the feed injection point) is ~ 0.4, δU^* is poorest. In this instance, δU^* is largest for cuts either near 0.1 or between ~ 0.7 and 0.8.

The contour representations of $\delta U^*(\alpha,\beta)$, which contain the same information and are obtained from the $\delta U^*(L,\theta)$ plots, also reflect the effect of axial variation of the circulatory flow. The δU^* contours in Figure 2 slope gently downward as β increases (or, according to Eq. (3), as θ increases). The δU^* terrain in Figure 3 is about twice as steep as it is in Figure 2 but slopes in the same direction. The contour plot for case C (Figure 4) has a distinctly different character from those of the previous two cases. Large δU^* values are achieved for both combinations of large α, small β and for small α, large β. At high flow rates (near the $L = L_{max}$ boundary), δU^* is depressed near the symmetry line ($\alpha = \beta$).

3. Cascade Design

In this section, constant-α and variable-α ideal cascades constructed of centrifuges with performance functions represented by Figures 2 - 4 are compared. Comparison is based upon the unit cost of product of a specified composition. It is assumed that all costs are proportional to the total number of centrifuges in the cascade, so that the unit product cost is:

$$C_p(\$/\text{kg UF}_6) = k \sum_1^n c_i \Big/ P \tag{7}$$

where k is the annual cost of operating one centrifuge (including capital recovery, machine replacement, power and operating costs) and c_i is the number of centrifuges in stage i. The cascade contains n stages and P is the product flow rate from the top stage. The quantity by which a particular cascade design is judged is the ratio C_p/k, which, according to Eq. (7), is equal to the number of centrifuges in the cascade divided by the product flow rate. This comparison is meaningful only

if the two cascades under consideration receive feed of the same composition and produce waste and product streams of the same assay.

In designing a variable-α cascade, the separation factors at each stage are selected in a manner which minimizes the product cost C_p. However, in order to satisfy the requirement of no mixing, the heads and tails separation factors on adjacent stages must satisfy the condition (see Appendix II):

$$\alpha_{i-1} = \beta_i \tag{8}$$

A method of designing a no-mixing cascade which satisfies this restraint is presented in Appendix III. For any specified set of heads separation factors (i.e., $\alpha_0, \alpha_1, \ldots\ldots\alpha_n$), the throughput to the centrifuges in stage i follows from the performance function and Eq. (8), namely, $L_i = L^*(\alpha_i, \alpha_{i-1})$. The performance function $L^*(\alpha,\beta)$ is obtained from one of the contour plots of Figures 2, 3, or 4 by dividing δU^* by $f(\alpha,\beta)$ given by Eq. (4). Similarly, the cut of the centrifuges in stage i is found by combination of Eqs. (3) and (8).

In order to assure integer numbers of stages in the stripping and enriching sections and to avoid isotope mixing with natural uranium feed, the waste and product compositions cannot be specified a priori. Instead, these compositions are chosen to be as close as possible to nominal values of 0.003 and 0.03 respectively when the number of stages in each section are integers. The unit product cost of the variable-α cascade is then determined from Eq. (7). This quantity depends only upon the separation factors assigned to each stage and the performance function of the centrifuges in the cascade.

If the separation factor is to be the same at all stages of an ideal cascade, Eq. (8) shows that α must be equal to β. In terms of the contour plots, α (and β) must lie along the 45° lines in Figures 2 - 4. For all three centrifuges, maximum separative power along the symmetry lines occurs at the

largest allowable flow rate. (This feature may not occur if the effect of feed on the velocity profiles is incorporated into the centrifuge performance model). The maximum δU^* for the constant-α cascades are denoted by the points marked "S" in Figures 2 - 4. The unit product cost for the constant-α cascade may be determined from conventional ideal cascade theory (2). For each performance function there is only one minimum product cost constant-α cascade. There are, on the other hand, an infinite number of variable-α cascades. The "savings":

$$\text{savings}(\%) = \frac{(C_p)_{\text{const.}-\alpha} - (C_p)_{\text{vbl.}-\alpha}}{(C_p)_{\text{const.}-\alpha}} \times 100 \tag{9}$$

is the measure of the superiority (or inferiority) of a particular variable-α cascade design over the best possible constant-α mode of operation of the available centrifuges. The unit product cost of the constant-α cascade is evaluated at the same feed, product, and waste compositions as those of the particular variable-α cascade with which comparison is made.

The remaining question is how to select the set of heads separation factors for the variable-α cascade in a manner which minimizes C_p. For guidance to the solution of this problem, we utilize the performance function plots. Eq. (8) indicates that the heads separation factor of a stage in an ideal cascade must be equal to the tails separation factor of the stage above it. One method of selecting a set of α_i values is to require that for each β, the corresponding α be chosen as the point on the contour plot for which δU^* is a maximum. This specification defines an "operating line" on the contour plot, to which the conditions of all stages in the cascade are restricted.

The Type-A Centrifuge

The operating line delineating the "ridge" of separative power for the Type-A centrifuge is shown in Figure 2. Suppose the first stage is operated at the point A in the plot ($\alpha_1 = 1.40$, $\beta_1 = 1.17$). The cascade condition given by Eq. (8) requires that $\beta_2 = \alpha_1 \doteq 1.40$. The point on the operating line corresponding to $\beta_2 = 1.40$ is $\alpha_2 = 1.17$ (Point A' of Figure 2). The separative power of the A' stage is smaller than that of the A stage. Because the operating line is symmetric about the 45° line, all odd number stages operate with the centrifuges at point A and all even number stages consist of centrifuges with the characteristics of point A'. This arrangement produces the following set of heads separation factors which constitute the input information to the variable-α cascade analysis:

$$\beta_1 = \alpha_0 = 1.17$$
$$\alpha_1 = 1.40$$
$$\alpha_2 = 1.17$$
$$\alpha_3 = 1.40$$
$$\vdots$$

Calculation of the unit product cost for this particular variable-α design and for the constant-α design corresponding to the point S on Figure 2 shows that the savings defined by Eq. (9) is -3.7%. That is, the variable-α design is less efficient than the conventional constant-α design. It does not matter whether the first stage is selected at A' or A. The same negative saving of -3.7% is found for the variable-α consisting of the points B and B' as well. The unit product cost of the constant-α cascade at point C in Figure 2 is also

3.7% greater than that of the point S cascade. For the type-A centrifuge, there does not appear to be any way of designing a variable-α cascade which is superior to the constant-α cascade composed of centrifuges each of which operates at its maximum separative power (point S). Although the separative powers of the stages operated at points A or B are greater than the separative power at S, the stages which must operate at points A' and B' produce less separative work than machines operating at S. The net result is that the loss of separative work due to the high-cut operation at A' or B' more than offsets the gain in separative performance arising from the low-cut operation of the machines at A or B.

The Type-B Centrifuge

The variable-α cascade composed of Type-B centrifuges most likely to compete successfully with the best constant-α design follows the operating line shown in the contour plot of Figure 3. The first stage of the variable-α cascade has been arbitrarily selected at the point $\alpha_1 = 1.52$, $\beta_1 = 1.07$. Once this point has been chosen, the operating points of the remaining stages are fixed by the operating line and the cascade condition of Eq. (8). The operating points for the 11 stages in the variable-α cascade are shown as the numbered dots along the operating line in Figure 3. Note that because the operating line is not symmetric about the 45° line, operating conditions closer to symmetry are approached towards the top of the cascade. The unit product cost calculated for this particular variable-α design is 5.4% greater than that obtained for the

constant-α cascade operated at point S in Figure 3. For this particular centrifuge performance function, there does not appear to be a better way of designing a cascade then as a conventional constant-α assembly of centrifuges operating at maximum separative power.

The Type-C Centrifuge

The contour plot of Figure 4 for the Type-C centrifuge does not exhibit a ridge of δU^* of approximately hyperbolic shape in the α-β plane as do the Types A and B centrifuges. Instead, the separative power in the region of symmetric operation is lower than the δU^* on the heights at either side of the 45° line. Consequently, we have selected a variable-α cascade whose stage operating points oscillate between points A and A' in Figure 4 for comparison with the best constant-α cascade at point S. If the first stage is selected at point A, all odd numbered stages operate with $\alpha = 1.50$, $\beta = 1.08$. For the even numbered stages (point A'), $\alpha = 1.08$, $\beta = 1.50$. The average separative of the powers at points A and A' is larger than the maximum separative power along the symmetry line (point S). The detailed cascade analysis described in Appendix D shows that the savings is 5.5% if stage one is at point A and 5.7% if the cascade is started at point A'.

Figure 5 shows the details of the variable-α cascade of Type-C centrifuges in which the odd-numbered stages are represented by point A' in Figure 4 and the even-numbered stages operate at point A. The ordinate height of each stage in Figure 5 gives the heads concentration leaving the stage and the width of the rectangles is proportional to the number of centrifuges in the stage. The heavy vertical arrows represent large flow rate streams (heads flow from high-cut stages and tails flow from low-cut stages) and the light arrows indicate small flow rates. The cascade contains two stripping stages and six enriching stages

and supplies a product stream of slightly larger assay than the nominal requirement of 3%. The tails stream is somewhat more depleted than the desired waste composition of 0.3%.

The constant-α cascade to which the arrangement shown in Figure 5 was compared to obtain the 5.7% product unit cost saving cannot be diagrammed; for the same product and waste compositions as shown in Figure 5, noninteger numbers of stages would be required in a constant-α cascade with all stages represented by point S in Figure 4. However, the nearest integer stage cascade in which each centrifuge operates at point S of Figure 4 (α = 1.152) is shown in Figure 6. This cascade contains $\sim$ 5 times as many centrifuges as the one in Figure 4 but supplies $\sim$ 5 times the product flow rate as does the latter. The number of centrifuges per unit product flow rate is approximately the same for both arrangements. Despite the very different appearances of the variable-α cascade of Figure 5 and the constant-α arrangement in Figure 6, both cascades utilize the same centrifuges.

4. Separative Power and Value Function of Asymmetric Elements

The great utility of the Cohen value function given by Eq. (III-18) is that when used to calculate the separative duty ΔU of a cascade by Eq. (III-17) and to calculate the separative power of a single centrifuge by:

$$\delta U = L[\theta V(x_p) + (1-\theta)V(x_w) - V(x_F)], \qquad (10)$$

the ratio $\Delta U/\delta U$ is equal to the total number of centrifuges in the cascade, which is a direct measure of the cost of the process. This important result can be rigorously demonstrated only for ideal cascades consisting of symetrically operated centrifuges (i.e., for constant-α cascades). In the case of the variable-α cascade, in which δU is different for the centrifuges on each stage, the analog of Eq. (III-20) is:

$$\Delta U = \sum_{1}^{n} c_i \, \delta U_i \tag{11}$$

where ΔU is given by Eq. (III-17) and δU_i is the Cohen separative power (Eqs. (4) and (6)) for each of the c_i centrifuges comprising stage i of the cascade. We have not been able to prove that Eq. (11) is applicable to any variable-α, ideal cascade. However, Eq. (11) has been applied to the cascade shown in Fig. 5 using the interstage flow rates supplied by the detailed cascade analysis, and was found to be satisfied as accurately as the computations permitted.

The usefulness of Eq. (11) for symmetric cascades lies in the fact that the δU_i are the same for all centrifuges, thus providing a means of calculating the total number of centrifuges needed without a complete cascade analysis. For the variable-α cascade, on the other hand, Eq. (11) does not permit computation of the total number of centrifuges, which can be obtained only by the methods outlined in Appendix III.

Bulang's (6) analysis of the asymmetric element produces, in addition to the separative power of Eq. (5), an associated value function. Unfortunately, this value function depends upon α and β as well as upon concentration. Consequently, a value balance over a variable-α cascade cannot be made because there is no way of deciding which of the many α's to use in the value functions in (Eq. (III-17)).

5. Conclusions

It has been shown that it is possible to design ideal cascades wherein the separation factors vary in an arbitrary fashion with stage number. For certain types of centrifuge performance functions, a properly chosen set of heads separation factors results in a cascade for which the product has a lower unit cost than any constant-α cascade utilizing the same centrifuges and producing the same exit stream compositions. The separative power of the asymmetrically

operated centrifuge in a variable-α cascade is a useful guide to the efficiency of the cascade design; the unit cost of product is lowest when the average δU^* of the stages in the cascade is largest. When the restriction of constant separation factor at each stage is removed, the search for the most efficient cascade can be reduced to the following topological problem: to find the set of points (α_i, β_i), $i = 1, \ldots, n$, on the performance function contour plot which maximizes δU^*_{avg} subject to the restraint $\alpha_{i-1} = \beta_i$.

Despite the greater flexibility that removal of the restriction of symmetric operation provides in cascade design, not all types of centrifuge can be arranged in variable-α cascades which are better than the conventional constant-α cascade. Variable-α designs appear to be superior to constant-α designs only when the centrifuge exhibits a minimum in the circulatory flow near the midplane of the rotor. However, the general question of the character of the internal flow profile which produces performance functions from which efficient variable-α cascades can be constructed has not been explored in detail. Only the three axial decay shapes shown in Figure 1 and analyzed by the Cohen model were investigated in this work. Nor has the question of how to deduce the set of separation factors which yield the most efficient ideal cascade for a given performance function plot been investigated in detail.

Despite these unexplored areas, the present calculations have demonstrated that for at least one type of performance function, cascades should be constructed with variable rather than constant separation factors at each stage. Determination of the performance function of a particular centrifuge (i.e., one of specified rotor geometry and peripheral speed) either theoretically or experimentally is a tedious job, primarily because of the necessity of optimizing the performance function with respect to all internal variables which can affect the gas circulation inside the rotor. The cost of obtaining the performance function $\delta U^*(L,\theta)$ must be justified in terms of the potential benefits of more efficient cascade performance. The savings of $\sim$ 5% found for the Type-C centrifuge in this work can be translated into a cost saving in the following way. The annual separative work capacity

which will be required in the United States in the next 50 years has been estimated to be between 100 and 400 million SWU/yr, depending upon the date of introduction of LMFBRs (8). The specific cost of plants constructed in this time period will probably be between $130 and $200 per SWU/yr capacity (9). Thus, the investment in isotope separation plants up to the year 2020 will be between 13 and 80 billion dollars. If all of this capacity is in the form of centrifuges, a 5% improvement in efficiency represents a saving of between 2/3 and 4 billion dollars. There appears to be ample incentive to justify exploring all proposed centrifuge designs for the possibility of cost reduction by use in ideal cascades with variable separation factors.

Acknowledgement

Part of this work was carried out under the auspices of the U. S. Atomic Energy Commission.

APPENDIX I

CENTRIFUGE PERFORMANCE MODELS

Within the context of the Cohen model (1), the change in the U-235 concentration with axial position in the rotor is given by Eqs. (52) and (59) of Reference 3. The effect of throughput on the velocity distribution is neglected in the analysis and the axial gradient equations are:

$$\frac{1}{g}\frac{dx}{d\eta} = x - \gamma\theta L(x_p - x) \tag{I-1}$$

in the enricher, and:

$$\frac{1}{g}\frac{dx}{d\eta} = x - \gamma(1 - \theta)L(x - x_w) \tag{I-2}$$

in the stripper. In these equations, η is the axial position in units of rotor length and x is the isotopic fraction of U-235 in the gas at position η. The coefficients g and γ, which may depend upon η, are given by:

$$\frac{1}{\gamma(\eta)} = 2a^2 \int_0^{r_2} F(r,\eta)\, r dr \tag{I-3}$$

and

$$\frac{1}{g(\eta)} = \gamma(\eta) \left\{ \frac{1}{2}(2\pi\rho D r_2) + \frac{\int_0^1 [F(r,\eta)]^2\, dr/r}{(2\pi\rho D r_2)} \right\} \frac{1}{(Z/r_2)} \tag{I-4}$$

where Z and r_2 are the length and radius, respectively, of the rotor and ρD is the density-diffusivity product of UF_6 gas. The constant a^2 is:

$$a^2 = \frac{\Delta M \Omega^2}{2RT} \tag{I-5}$$

where $\Delta M = 3$ is the mass difference between the two uranium isotopes, Ω is the angular speed of the rotor, R is the gas constant and T is the temperature of the bulk gas in the centrifuge. $F(r,\eta)$ is the flow function, defined by:

$$F(r,\eta) = 2\pi \int_0^r \rho w(r',\eta) r' dr' \tag{I-6}$$

$w(r,\eta)$ is the axial component of the gas velocity in the rotor.

A. Nondecaying Flow

If w is not a function of η, g and γ are constants. Eqs. (I-3) and (I-4) may be written as:

$$\frac{1}{\gamma} = \frac{1}{\sqrt{2}} (a^2 r_2^2) \sqrt{E} (2\pi\rho D r_2) m \tag{I-7}$$

$$g = \frac{1}{\sqrt{2}} (a^2 r_2^2) \sqrt{E} \left(\frac{Z}{r_2}\right) \left[\frac{2m}{1 + m^2}\right] \tag{I-8}$$

where E is the flow pattern efficiency:

$$E = \frac{4}{r_2^4} \frac{\left[\int_0^{r_2} F(r)\, r dr\right]^2}{\int_0^1 [F(r)]^2\, dr/r} \tag{I-9}$$

and m is a dimensionless quantity dependent upon the magnitude of the internal flow:

$$m = \frac{\left\{2 \int_0^{r_2} [F(r)]^2\, dr/r\right\}^{1/2}}{(2\pi\rho D r_2)} \tag{I-10}$$

with g and γ constant, Eqs. (I-1) and (I-2) may be integrated analytically (3). Using the definition of the heads and tails separation factors given by Eqs. (1) and (2), there results:

$$\alpha = \frac{(1 + \theta\gamma L)\ \exp[g(1 - \eta_F)(1 + \theta\gamma L)]}{1 + \theta\gamma L\ \exp[g(1 - \eta_F)(1 + \theta\gamma L)]} \tag{I-11}$$

$$\beta = \frac{\exp\{g\eta_F[1 - (1 - \theta)\gamma L]\} - (1 - \theta)\gamma L}{1 - (1 - \theta)\gamma L}$$

where η_F is the axial position at which the concentration is equal to x_F. The feed point is assumed to be adjusted to prevent isotope mixing by feed injection. Elimination of η_F between Eqs. (I-11) and (I-12) yields:

$$\frac{\alpha}{1 - (\alpha - 1)\theta\gamma L} = \exp\left\{g(1 + \theta\gamma L)\left[1 - \frac{\ln[\beta - (\beta - 1)(1 - \theta)\gamma L]}{g[1 - (1 - \theta)\gamma L]}\right]\right\} \tag{I-13}$$

The cut may be eliminated from Eq. (I-13) by use of Eq. (3), which yields an equation which may be solved numerically for the throughput L as a function of α, β, g and γ. Since all of the terms in Eqs. (I-7) and (I-8) except m are fixed once the rotor speed, radius and height are specified, we have L as a function of α, β, and m. $L^*(\alpha,\beta)$ is determined from this equation by maximizing L with respect to m. Finally, the performance function $\delta U^*(\alpha,\beta)$ is determined by use of Eqs. (4) and (5). The alternate performance function, $\delta U^*(L,\theta)$, may be constructed directly from these results. The numerical work, the coefficient of m in Eq. (I-7) was taken as 60 and the coefficient of the bracketed function of m in Eq. (I-8) was assumed to be 1.8.

B. Flow Decay from One End

The circulatory flow in a centrifuge can be driven by a temperature difference ΔT_h between a heated end cap and the bulk gas. The axial velocity profile generated by this driving mode is represented by the product of a radial shape function and an exponential decay from the heated end plate ($\eta = 0$):

$$w(r,\eta) = \Delta T_h \, h(r) \, e^{-\kappa\eta} \tag{I-14}$$

The function h(r) specifies the radial shape and magnitude of the velocity. The flow magnitude is proportional to the temperature driving force ΔT_h, which has been extracted from h(r) because of its role as the internal variable used for optimization. The radial function h(r) has been taken from the work of Jacques (4). When Eq. (I-14) is used in Eq. (I-6) and the resulting flow function inserted in Eqs. (I-3) and (I-4), the axial dependence of the coefficients g and γ in the gradient equations is fixed. Eqs. (I-1) and (I-2) are integrated numerically. Eq. (I-2) is employed from $\eta = 0$ to the position at which the computed concentration is equal to x_F. Thereafter, numerical integration continues using Eq. (I-1) until $\eta = 1$ is attained. In the computations, a value of $\kappa = 1.5$ was used.

C. Flow Decay from Both Ends

If one end plate of a centrifuge is maintained hotter than the bulk gas and the other end plate is cooled, the flows generated at each end cause circulation in the same direction in the rotor. The axial velocity profile may be obtained by superposition of the flows generated by each end plate:

$$w(r,\eta) = h(r) \left[\Delta T_h e^{-\kappa\eta} + \Delta T_c e^{-\kappa(1-\eta)} \right] \tag{I-15}$$

The flow decays from each end towards the midplane of the rotor. The internal variables of the centrifuge are the two temperature differences ΔT_h and ΔT_c and optimization should be performed on both of them. However, we have arbitrarily fixed the ratio of ΔT_c to ΔT_h at 2.23 and optimized only upon ΔT_h. The decay constant κ was also arbitrarily chosen equal to 4 to produce a factor of two decrease in the flow magnitude between the hot end and the midplane of the centrifuge.

APPENDIX II

RELATION BETWEEN THE HEADS AND TAILS SEPARATION FACTORS IN AN IDEAL CASCADE

Figure 7 shows two stages of a recycle cascade in which the heads stream from stage i-1 is fed to stage i and the tails stream from stage i-1 constitutes the feed to stage i-2. For the limiting case of U-235 fractions much less than unity, the requirement of no isotope mixing leads to:

$$u_{i-2} = v_i \tag{II-1}$$

where u_i and v_i are the heads and tails concentrations, respectively, in the streams leaving stage i. The heads separation factor for stage i-1 is:

$$\alpha_{i-1} = u_{i-1}/u_{i-2} \tag{II-2}$$

The tails separation factor for stage i is:

$$\beta_i = u_{i-1}/v_i \tag{II-3}$$

Substituting Eqs. (II-1) and (II-2) into (II-3) yields:

$$\alpha_{i-1} = \beta_i \tag{II-4}$$

The cut at stage i is given by Eq. (3) which, when combined with Eq. (II-4) results in:

$$\theta_i = \frac{\alpha_{i-1} - 1}{\alpha_i \alpha_{i-1} - 1} \tag{II-5}$$

APPENDIX III

NO-MIXING, VARIABLE-α CASCADE ANALYSIS

We wish to determine the product flow rate, the number of stages and the number of separating units per stage in a cascade subject to the following restraints:

1. The feed to the cascade is natural uranium ($X_F = 0.0071$). Nominal product and waste compositions are 0.03 and 0.003, respectively. Exact values of X_p and X_w are to be chosen so that they are as close to the nominal values as possible and: (a) the cascade contains an integer number of stages; (b) the composition at the feed stage is exactly equal to 0.0071.
2. The heads and tails from each stage flow to the adjacent upper and lower stages, respectively.
3. No mixing of streams of different isotopic composition occurs anywhere in the cascade.
4. All U-235 isotopic fractions are negligible compared to unity.
5. Each separating unit in the cascade has the same performance function $L^*(\alpha,\beta)$, which may be obtained from $\delta U^*(\alpha,\beta)$ plots such as those of Figures 2 - 4 by use of Eqs. (4) and (5). The separating units in each stage operate identically. However, each stage need not be operated at the same values of α and β as the other stages (i.e., the cascade is not necessarily a constant-α cascade).
6. The heads separation factor of each stage in the cascade is assumed to be specified. In addition, the tails separation factor for the bottom stage in the stripping section is specified.

We define a "minimum" cascade which supplies a product flow rate P from a single separating unit comprising the top stage. A cascade to supply a production rate larger than P may be regarded as composed of the appropriate number of minimum cascades.

The material balance over the enriching section of a recycle cascade constructed according to specification 2 above is (2):

$$u_i - v_{i+1} = \frac{X_p - u_i}{N_{i+1}/P} \qquad \text{(III-1)}$$

where N_i is the total tails flow rate from stage i. If L_i is the throughput to each separating unit in stage i and c_i is the number of separating units connected in parallel at stage i:

$$N_i = c_i(1-\theta_i)L_i \qquad \text{(III-2)}$$

The cut at stage i, θ_i, may be eliminated by use of Eq.(III-5), and substitution of Eq. (III-2) into Eq.(III-1) yields:

$$u_i - v_{i+1} = \frac{P}{L_{i+1}} \frac{\alpha_{i+1}\alpha_i - 1}{\alpha_i(\alpha_{i+1} - 1)} \frac{X_p - u_i}{c_{i+1}} \qquad \text{(III-3)}$$

Let the cascade contain n stages. At the n'th stage, $c_n = 1$ and:

$$P = \theta_n L_n = \left(\frac{\alpha_{n-1} - 1}{\alpha_n \alpha_{n-1} - 1}\right) L_n \qquad \text{(III-4)}$$

The product flow rate P may be eliminated from Eq.(III-3) by use of Eq.(III-4) The tails concentration at stage i+1 may be removed from Eq.(III-3) by using the no mixing requirement, $v_{i+1} = u_{i-1}$. With these substitutions, Eq. (III-3) may be solved for c_{i+1}:

$$c_{i+1} = \frac{L_n}{L_{i+1}} \left(\frac{\alpha_{i+1}\alpha_i - 1}{\alpha_n \alpha_{n-1} - 1}\right)\left(\frac{\alpha_{n-1} - 1}{\alpha_{i+1} - 1}\right) \frac{1}{\alpha_i} \frac{X_p - u_i}{u_i - u_{i-1}} \qquad \text{(III-5)}$$

Since the performance function $L^*(\alpha,\beta)$ is the same for all separating units, and according to Eq.(III-4) $\beta_i = \alpha_{i-1}$, the flow rate L_i is determined by the heads separation factors of stages i and i - 1:

$$L_i = L^*(\alpha_i, \alpha_{i-1}) \tag{III-6}$$

Using Eq.(III-6) (and the analogous relation for the top stage), Eq.(III-5) becomes:

$$c_i = \frac{L^*(\alpha_n, \alpha_{n-1})}{L^*(\alpha_i, \alpha_{i-1})} \left(\frac{\alpha_i \alpha_{i-1} - 1}{\alpha_n \alpha_{n-1} - 1}\right) \left(\frac{\alpha_{n-1} - 1}{\alpha_i - 1}\right) \frac{1}{\alpha_{i-1}} \frac{X_p - u_{i-1}}{u_{i-1} - u_{i-2}} \tag{III-7}$$

Eq.(III-7) applies to the enriching section, $n_w + 1 \leq i \leq n$, where n_w is the number of stages in the stripping section and n is the total number of stages in the cascade. In the stripping section, $1 \leq i \leq n_w$, the number of separating units per stage is:

$$c_i = c_1 \frac{L^*(\alpha_1, \alpha_0)}{L^*(\alpha_i, \alpha_{i-1})} \left(\frac{\alpha_i \alpha_{i-1} - 1}{\alpha_1 \alpha_0 - 1}\right) \left(\frac{\alpha_1 - 1}{\alpha_{i-1} - 1}\right) \alpha_0 \frac{u_{i-1} - X_w}{u_i - u_{i-1}} \tag{III-8}$$

where:

$$c_1 = \left(\frac{X_p - X_F}{X_F - X_w}\right) \left(\frac{\alpha_{n-1} - 1}{\alpha_n \alpha_{n-1} - 1}\right) \left(\frac{\alpha_1 \alpha_0 - 1}{\alpha_0 (\alpha_1 - 1)}\right) \frac{L^*(\alpha_n, \alpha_{n-1})}{L^*(\alpha_1, \alpha_0)} \tag{III-9}$$

In Eqs.(III-8) and (III-9) the separation factor of the hypothetical zeroth stage, α_0, is equal to the tails separation factor of stage one, β_1.

The cascade gradient equation is:

$$u_{i+1} = \alpha_{i+1} u_i \tag{III-10}$$

With $\alpha_0, \ldots\ldots \alpha_n$ specified, the solution procedure is as follows: Starting from $i = 1$, where $u_1 = \alpha_1 \alpha_0 X_w$, Eq.(III-10) is integrated until $u_i = X_F$. X_w is adjusted about the nominal composition of 0.003 until the composition at the feed stage is exactly 0.0071. This procedure fixes X_w and n_w. Integration of Eq.(III-10) continues until the stage n at which the calculated heads composition is closest

to the nominal product composition of 0.03. The number of stripping and enriching stages and the product and waste compositions from the cascade are thus determined. In addition, u_i is known as a function of stage number.

With α_i specified at each stage and u_i known by the previous solution of the cascade gradient equation, the number of separating units in each stage is determined from Eqs. (III-7) and (III-8). In this calculation, the performance function is available (e.g., from Figures 2, 3, or 4). The number of separating units at each stage is not necessarily an integer, except for the product stage where $c_n = 1$.

Let k be the cost attributable to the capital investment and operating expenses of each separating unit, in dollars per separating unit per year. The total yearly cost of a cascade of n stages with c_i separating units per stage is:

$$C_{tot}(\$/yr) = k \sum_{1}^{n} c_i \qquad \text{(III-11)}$$

The cost per unit amount of product may be obtained by dividing C_{tot} by the product flow rate P. With the latter given by Eq. (III-4) and L_n expressed in terms of the performance function, we have:

$$C_p(\$/kg\ product) = k \left(\frac{\alpha_n \alpha_{n-1} - 1}{\alpha_{n-1} - 1} \right) \frac{\Sigma c_i}{L^*(\alpha_n, \alpha_{n-1})} \qquad \text{(III-12)}$$

Eq. (III-12) gives the unit cost of product from a variable-α ideal cascade providing a product of concentration X_p and a waste of composition X_w from a feed of composition $X_F = 0.0071$. The compositions X_p and X_w are close to 0.03 and 0.003, respectively; their exact values have been determined in the course of the computation.

In order to compare the variable-α cascade with the conventional constant-α cascade, the product cost of the latter must be calculated for the same product and waste compositions as those determined in the variable-α cascade analysis. For the case of constant separation factor, it may be shown that the equations derived above reduce to:

$$n = \frac{\ln(X_p/X_w)}{\ln\alpha} - 1 \qquad \text{(III-13)}$$

$$n - n_w = \frac{\ln(X_p/X_F)}{\ln\alpha} \qquad \text{(III-14)}$$

and:

$$\sum_1^n c_i = \frac{-P\ln(X_p/X_F) + W\ln(X_F/X_w)}{P(\alpha - 1)\ln\alpha} \qquad \text{(III-15)}$$

where:

$$\frac{W}{P} = \frac{X_p - X_F}{X_F - X_w} \qquad \text{(III-16)}$$

The numerator of Eq. (III-15) is the separative duty of the cascade defined in terms of the Cohen value function:

$$\Delta U = PV(X_p) + WV(X_w) - (P+W)V(X_F) \qquad \text{(III-17)}$$

where $V(x) = (2x-1)\ \ell n[x/(1-x)] \simeq -\ell nx$ (III-18)

Since $P = \Theta L = L/(1+\alpha)$, the denominator of Eq.(III-15) is the separative power of each separating unit (1):

$$(\delta U)_{sym} = \frac{L(\alpha-1)\ln\alpha}{\alpha+1} \qquad \text{(III-19)}$$

and the usual formula:

$$\sum_{1}^{n} c_i = \frac{\Delta U}{(\delta U)_{sym}} \tag{III-20}$$

is recovered. The unit product cost for the constant-α cascade is thus:

$$(C_p)_{sym} = k\,\frac{(\Delta U/P)}{(\delta U)_{sym}} = k\left\{\frac{-\ln\left(\frac{X_p}{X_F}\right) + \left(\frac{X_p - X_F}{X_F - X_w}\right)\ln\left(\frac{X_F}{X_w}\right)}{\frac{L^*(\alpha,\alpha)(\alpha-1)\ln\alpha}{\alpha+1}}\right\} \tag{III-21}$$

Comparison of the variable-α and constant-α ideal cascades involves evaluating the (C_p/k) values for each type. For the variable-α cascade, a series of heads separation factors, $\alpha_0, \ldots\ldots \alpha_n$ is selected from within the allowable cut and throughput ranges of the performance function. Exact values of X_p and X_w are calculated and the figure of merit C_p/k is computed from Eq. (III-12). For the constant-α cascade, the value of α which produces the largest separative power in symmetric operation is selected from the performance function plot. $(C_p/k)_{sym}$ is then calculated from Eq.(III-21) for this value of α and the values of X_p and X_w determined in the variable-α cascade analysis.

LITERATURE CITED

1. K. P. Cohen, "The Theory of Isotope Separation as Applied to the Large Scale Production of U-235", McGraw-Hill, New York (1951).

2. M. Benedict and T. H. Pigford, "Nuclear Chemical Engineering", Chapter 10, McGraw-Hill, New York (1957).

3. D. R. Olander, Adv. Nucl. Sci. & Tech. 6, 105 (1972).

4. R. Jacques, CEA Report R-4336 (1972).

5. J. Ging, U. S. AEC Report UVA-198-62S (1962).

6. W. Bulang, W. Groth, I. Jordan, W. Kolbe, E. Nann and K. H. Welge, Z. Phys. Chem. 24, 249 (1960).

7. C. Ouwerkerk and J. Los, U. N. Conf. on Peaceful Uses of At. Energy, 12, 367 (1964).

8. R. P. Omberg (HEDL), personal communication (1974).

9. ORO-735, USAEC (Nov. 1973).

FIGURE CAPTIONS

1. Variation of the magnitude of the circulatory flow (axial velocity component) with axial position in the rotor for three types of centrifuges.

2. The performance function for the Type-A centrifuge in terms of Bulang's separative power. The curves within the envelope of dashed lines represent contours at constant δU^*. The contour lines in the upper left hand corner of the envelope correspond to the large δU^* and those in the lower right hand corner are the smallest δU^*. The values of δU^* corresponding to each contour line differ by one swu/yr.

3. The performance function for the Type-B centrifuge in terms of Bulang's separative power. The curves within the envelope of dashed lines represent contours of constant δU^*. The contour lines in the upper left hand corner of the envelope correspond to the largest δU^* and those in the lower right hand corner are the smallest δU^*. The values of δU^* corresponding to each contour line differ by one swu/yr.

4. The performance function for the Type-C centrifuge in terms of Bulang's separative power. The small segments of contour lines near points A and A' represent the largest values of δU^*. The δU^* values associated with the remaining contour lines decrease towards the lower right hand portion of the envelope of dashed lines.

5. Variable-α cascade constructed of Type-C centrifuges.

6. Constant-α cascade constructed of Type-C centrifuges.

7. Three stages of a recycle cascade.

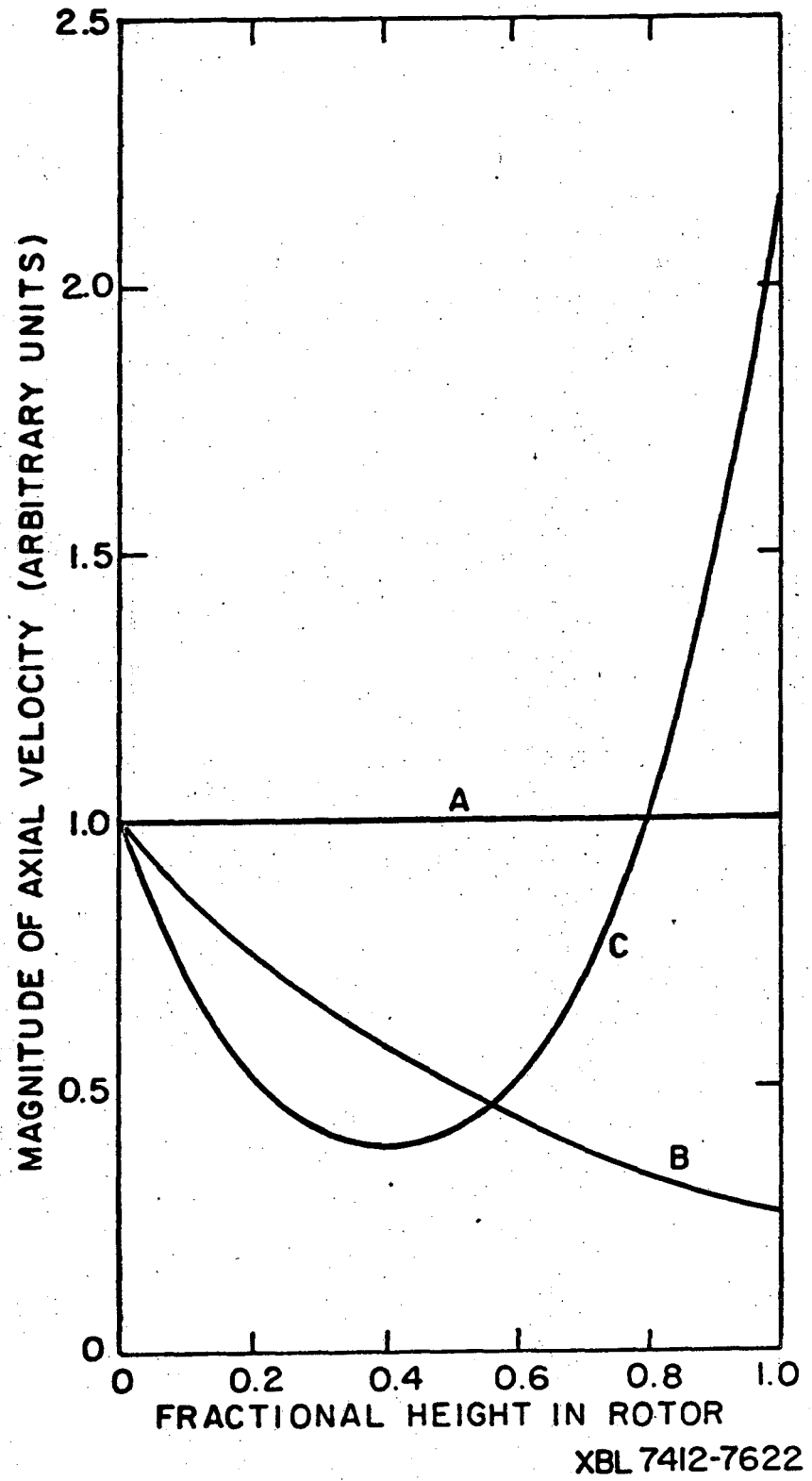
2.5
2.0
1.5
1.0
0.5
0
MAGNITUDE OF AXIAL VELOCITY (ARBITRARY UNITS)
A
B
C
0
0.2
0.4
0.6
0.8
1.0
FRACTIONAL HEIGHT IN ROTOR
XBL 7412-7622

Fig. 1

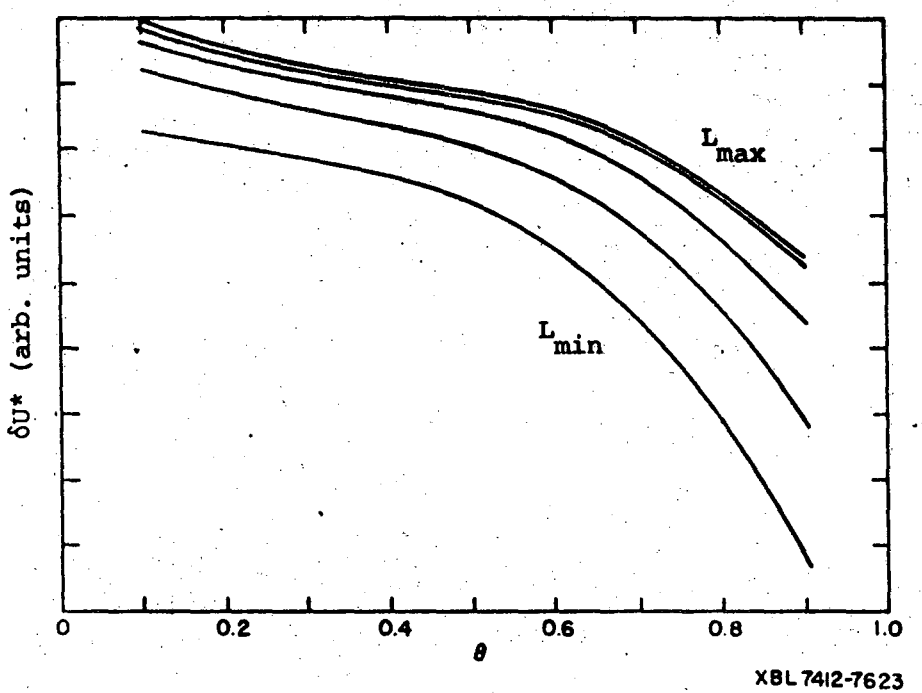
δU* (arb. units)
θ
0
0.2
0.4
0.6
0.8
1.0
L_{max}
L_{min}
XBL 7412-7623

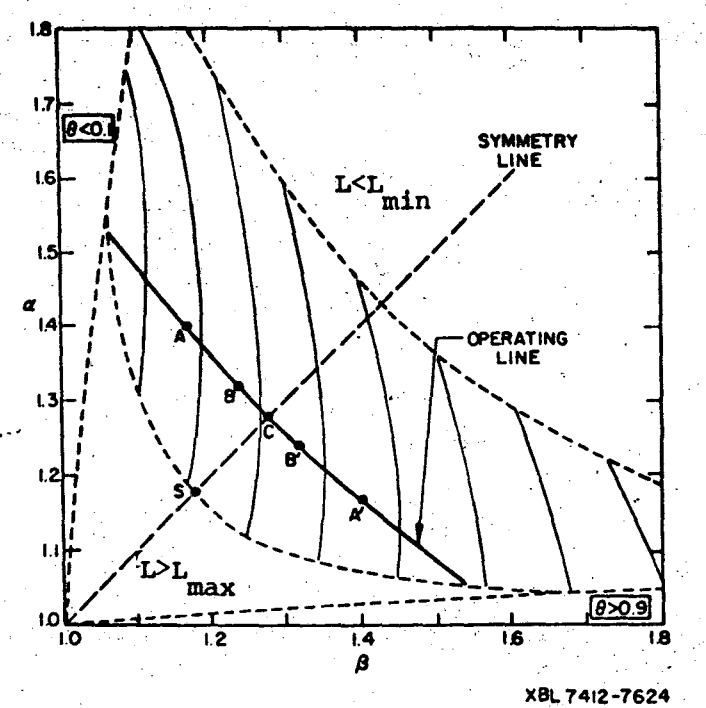
α
β
1.0
1.1
1.2
1.3
1.4
1.5
1.6
1.7
1.8
θ<0.1
θ>0.9
SYMMETRY LINE
$L<L_{min}$
OPERATING LINE
$L>L_{max}$
A
B
C
B'
A'
S
XBL 7412-7624

Fig. 2

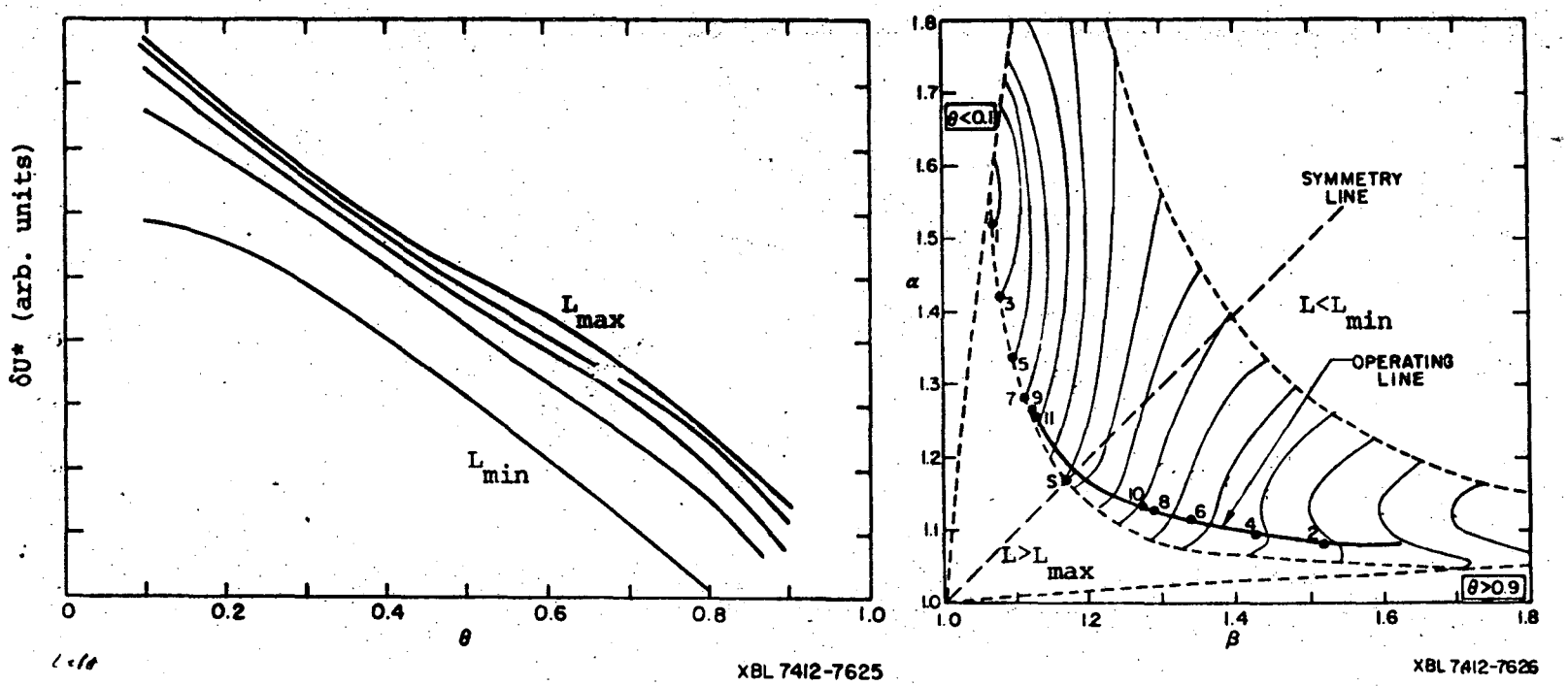
δU* (arb. units)
θ
0
0.2
0.4
0.6
0.8
1.0
L_max
L_min
XBL 7412-7625
α
β
1.0
1.1
1.2
1.3
1.4
1.5
1.6
1.7
1.8
θ<0.1
θ>0.9
SYMMETRY LINE
OPERATING LINE
L<L_min
L>L_max
XBL 7412-7626

Fig. 3

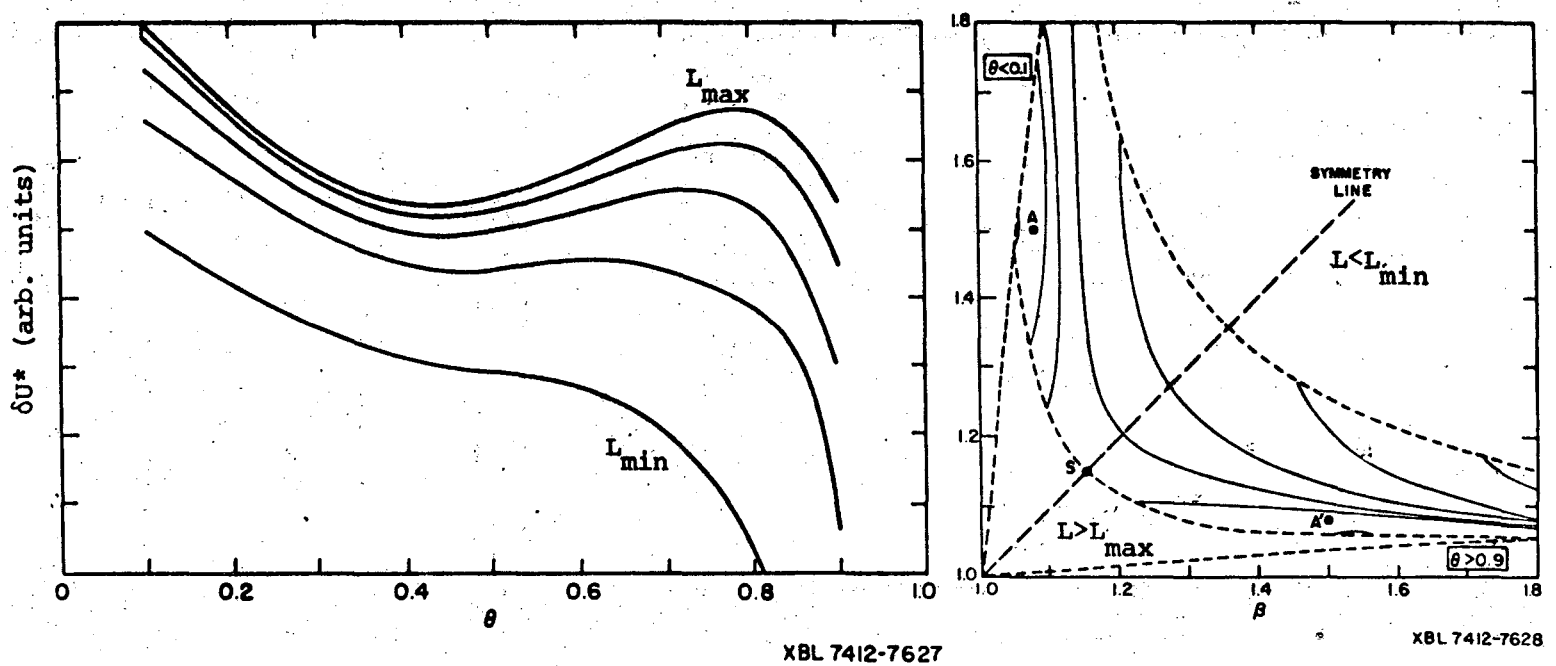

Fig. 4

0 0 0 0 4 2 0 7 8 3 0

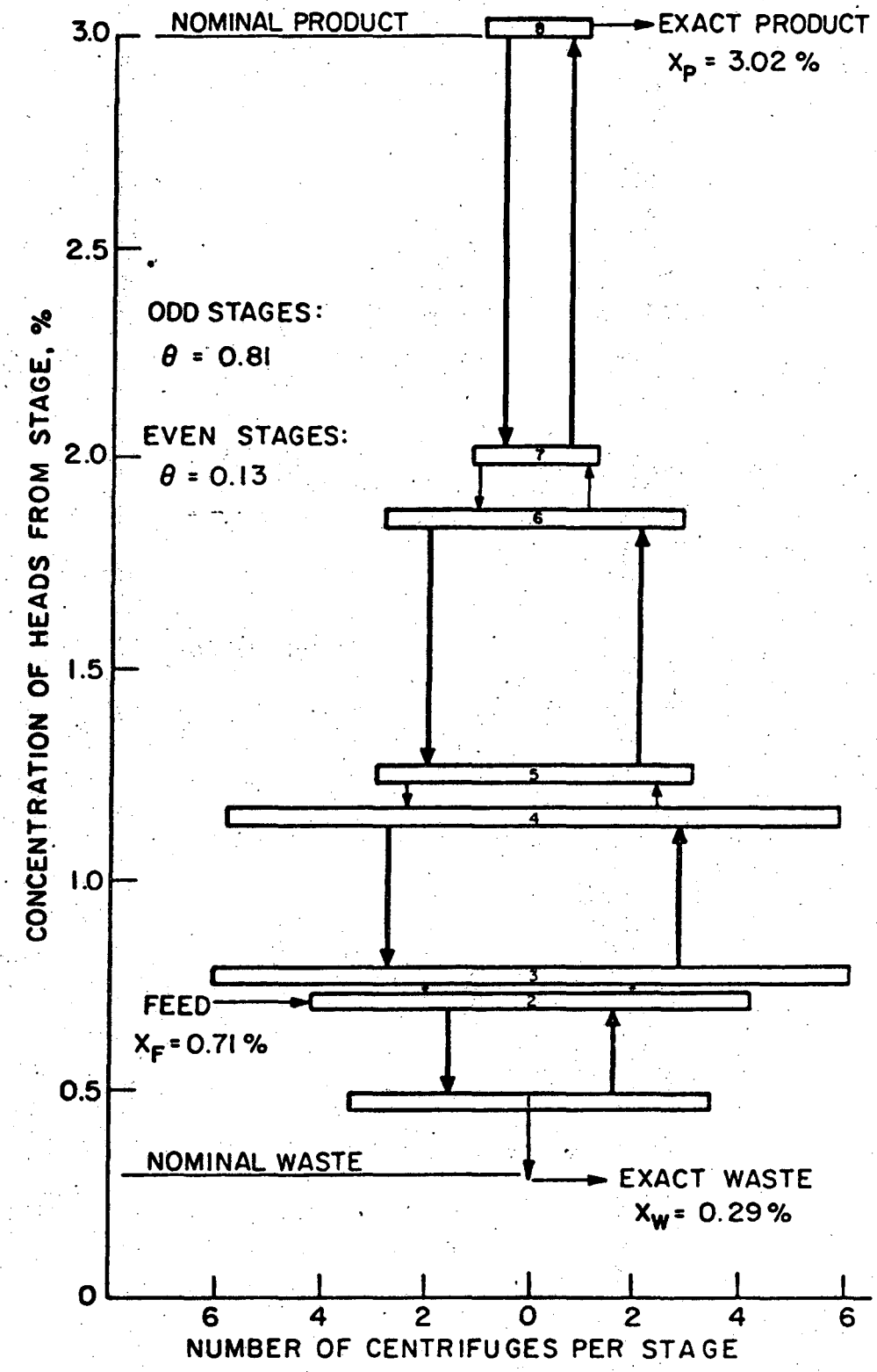

XBL 7412-7629

Fig. 5

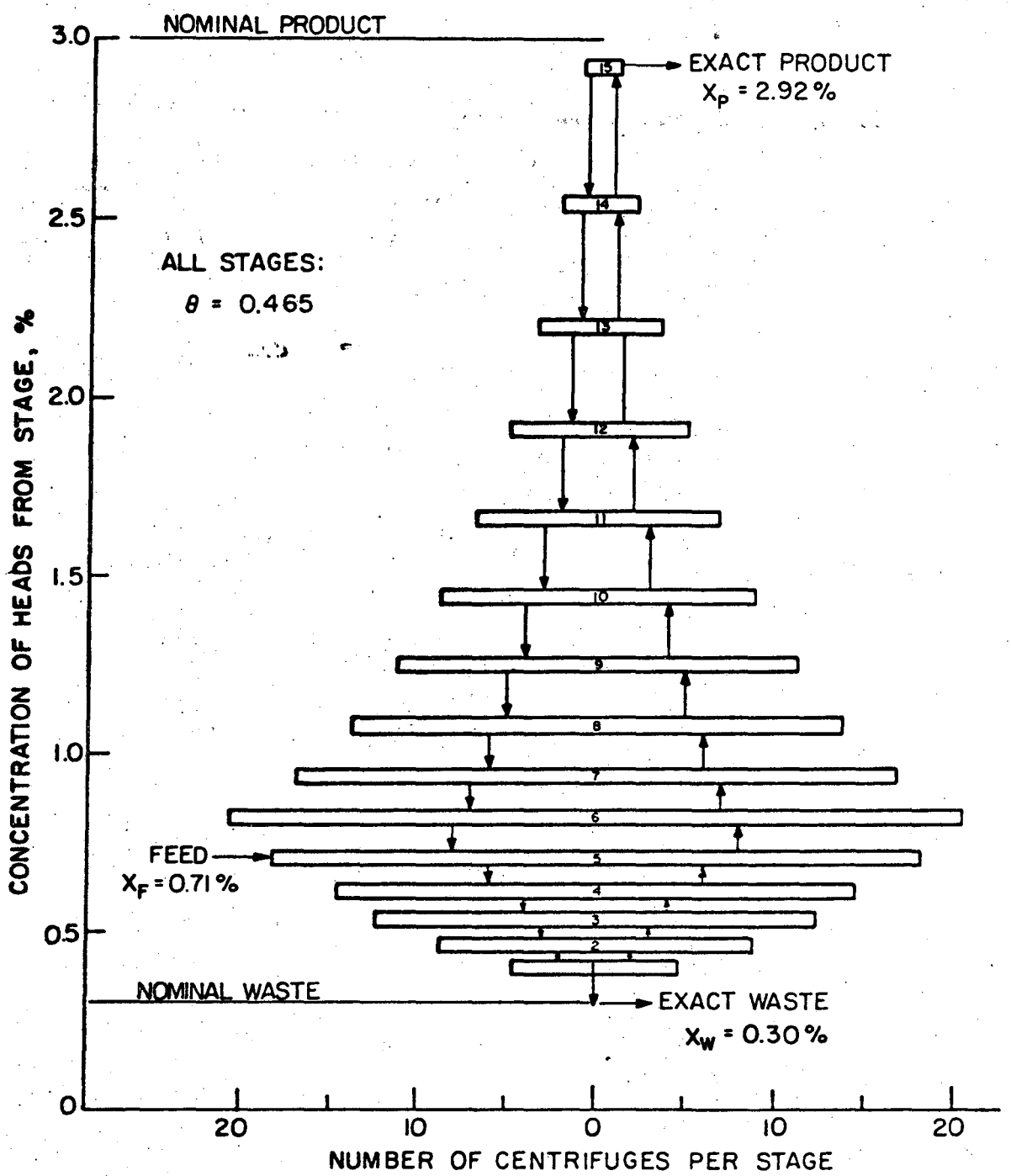

XBL7412-7630

Fig. 6

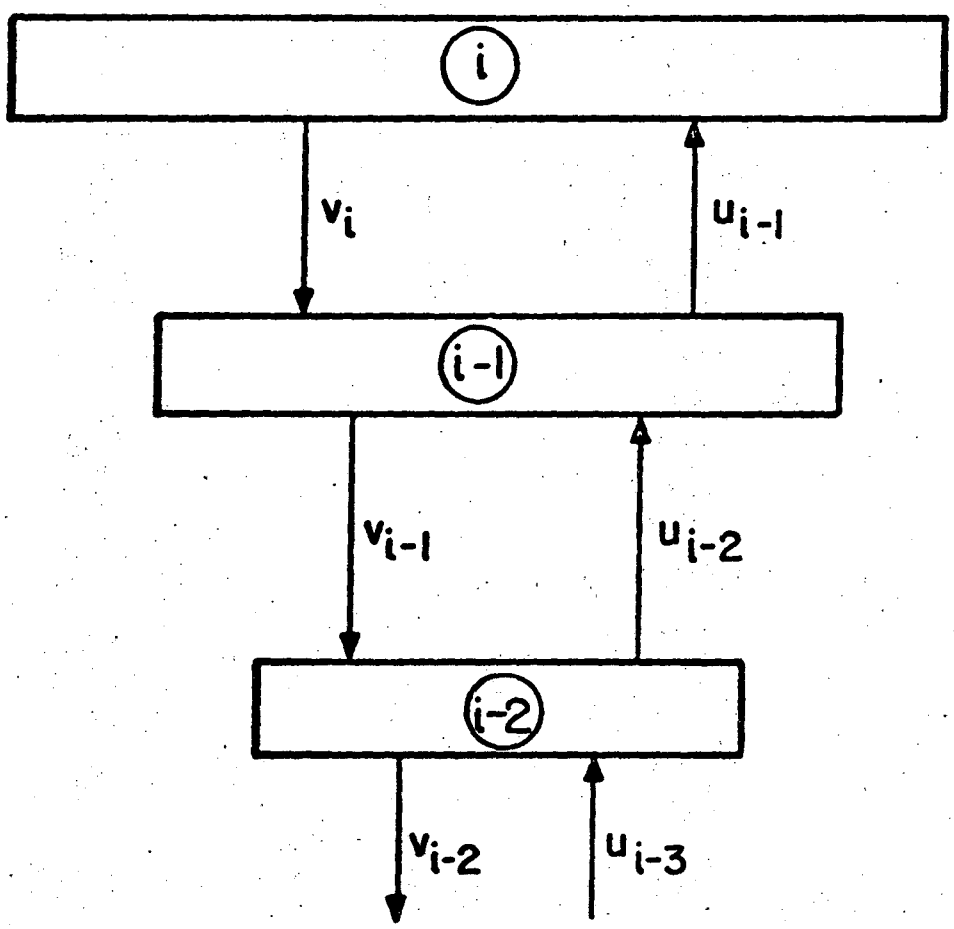

XBL 7412-7631

Fig. 7

0 0 0 0 4 2 0 7 8 3 2

LEGAL NOTICE

This report was prepared as an account of work sponsored by the United States Government. Neither the United States nor the United States Energy Research and Development Administration, nor any of their employees, nor any of their contractors, subcontractors, or their employees, makes any warranty, express or implied, or assumes any legal liability or responsibility for the accuracy, completeness or usefulness of any information, apparatus, product or process disclosed, or represents that its use would not infringe privately owned rights.

TECHNICAL INFORMATION DIVISION
LAWRENCE BERKELEY LABORATORY
UNIVERSITY OF CALIFORNIA
BERKELEY, CALIFORNIA 94720